Oleopneumatic Shock Strut Dynamic Analysis and Its Real-Time Simulation

Mahinder K. Wahi*
Boeing Commercial Airplane Company, Renton, Washington

An analog simulation representing dynamic shock absorption characteristics of a conventional oleopneumatic landing gear strut has been developed. This simulation includes both airplane and strut dynamics. The basic equations of motions are those used for a two-degree-of-freedom system. The hydraulic, pneumatic, and mechanical aspects of the shock strut dynamics have been analyzed. The metering orifice and snubber orifice discharge coefficients have been treated as a function of Reynolds number, orifice shape, and orifice orientation. The snubber valve hydraulic force during compression and rebound has been accounted for. Other factors considered in the system simulation are internal friction in the shock strut, wing lift, inclination of the landing gear, and the effects of wheel spinup and drag loads. A special circuit was devised on the analog simulation which allows the operator to vary the shape of the metering pin, observe the effects on shock strut load instantly, and optimize the load stroke curve(s). The simulation has the capability of high-speed, iterative operation. Good correlation has been established between flight/drop test data and the simulation predicted results. The simulation therefore provides an important design tool for optimizing pin profile, as well as evaluating existing shock strut designs.

Nomenclature

A_h = hydraulic area for the strut (inner cylinder area-metering pin area), in.^{2}
A_0 = cross-sectional area of an annular orifice, in.^{2} $A_0 = (\pi/4)(D^2 - d^2)$
A_p = cross-sectional area of the metering pin in plane of orifice
A_1 = internal cross-sectional area of inner cylinder, in.^{2}
A_2 = internal cross-sectional area of outer culinder, in.^{2}
C = overall annular orifice coefficient
C_c = coefficient of stream contraction in an orifice
C_d = coefficient or orifice discharge
D = o.d. of an annular orifice, in.
F = fraction of maximum pressure recovery due to stream expansion from the Vena Contracta to full annulus area actually recovered in a given orifice
F_s = total axial shock strut force, lb
G_0 = mass flow rate through an orifice, lb/(sec) (in.^{2})
K = number of velocity heads pressure drop due to kinetic energy effects in the viscous flow regime
L = orifice length, in.
Q = flow rate through orifice, in.^{3}/sec
Re = Reynolds number: circular orifice-$Re = D_0 G_0/\mu$; annular orifice-$Re = (D-d)G_0/\mu$
$\dot{S}$ = strut telescoping velocity, in./sec
V = velocity, in./sec
V_f = mean velocity of fluid through orifice, in./sec
W_0 = weight flow rate through an annular orifice, lb/sec
Z = concentric annulus length-to-width ratio
d = i.d. of an annular orifice, in.
f_p = friction factor for flow between parallel plates of infinite width
g_c = gravitational conversion constant: 386 (in.) (lb-mass) /(sec^2) (lb-force)
p = pressure, lb/(in.^{2})
p_a = air pressure in upper chamber of shock strut, psi
p_b = oil pressure in annular space between inner and outer cylinders, psi
p_h = oil pressure in lower chamber of shock strut, psi
Δp = pressure drop between two given points, lb/(in.^{2})
μ = fluid absolute viscosity at bulk temperature, lb/(in.) (sec)
π = numerical const, 3.14159
ρ = fluid density, lb/(in.^{3})
ρ_0 = fluid mass density, (lb-sec^2/in.^{4}
Z_1 = vertical displacement of upper mass from position at initial contact
Z_2 = vertical displacement of lower mass from position at initial contact
M_1 = upper or sprung mass
M_2 = lower or unsprung mass
F_f = frictional force in shock strut
F_{vg} = vertical force, applied to tire at ground
F_{Na} = force normal to axis of shock strut, applied at axle
Z = vertical axes, positive downward
X = horizontal axes, positive rearward
$(\dot{})$ = differentiation with respect to time t

Received December 9, 1974; revision received April 10, 1975. The author would like to acknowledge the very substantial assistance of the Boeing Commercial Airplane Company, who funded the research project. Thanks should also go to N. Attri and other colleagues, who provided valuable advice at various stages of the program.

Index Categories: Aircraft Landing Dynamics; Aircraft Subsystem Design; Computer Technology and Computer Simulation Techniques.

*Senior Engineer, Landing Gear Research.

Introduction

GENERALLY speaking, the analysis of a landing gear proceeds as follows: the actual mechanical system is idealized to a spring-mass damper system. Next, the expressions that account for the internal forces of the system as well as the external factors are formulated. The differential equations of motion of the system then are derived and solved by numerical integration procedures. It is on the point of force formulation that various analytical studies and some simplified model tests primarily differ from one another. Assumptions made include rigid or flexible airplane structure, compressible or incompressible fluid, isothermal to adiabatic exponent for air compression, discharge coefficients of 0.80 for one study to 1.25 for another, and so on. In the present analysis of the landing impact, the gear is treated as a single-degree-of-freedom system up to the instant of initial shock-strut deflection, after which it is considered as a system with two degrees of freedom. The equations for the system consider such factors as flow characteristics of annular orifices, of cylindrical tube orifices, internal friction in the shock strut, wing lift, inclination of the landing gear, and the effects of wheel spinup and drag loads.

The following sections will include a brief literature review and a general description of the simulation accompanied by block diagrams. This is followed by sample computer runs

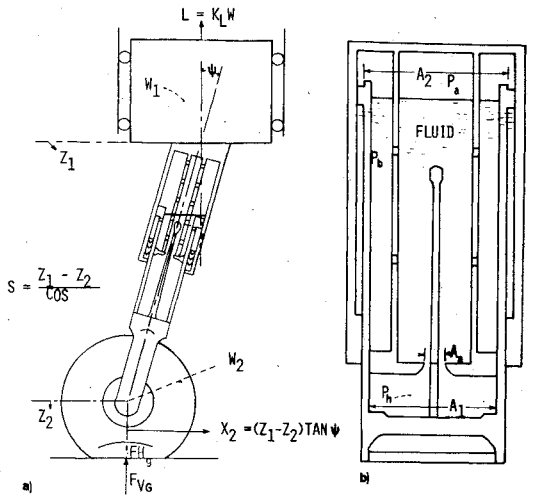

Fig. 1 Dynamical system considered in analysis. a) System with two degrees of freedom. b) Schematic representation of shock strut.

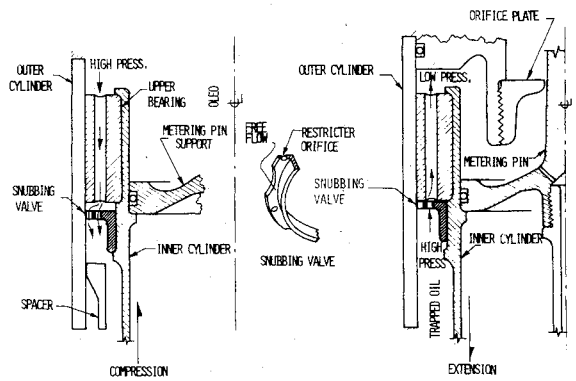

Fig. 2 Snubber orifice installation.

showing importance of various parameters established earlier and a direct comparison of simulation vs drop test data to establish the credibility of the analysis as well as simulation.

Literature Survey

Figure 1 shows a schematic representation of a typical oleopneumatic shock strut. A rebound control check valve, also called a snubber valve, incorporated into most shock struts as shown in Fig. 2. A study of various published[1-4] and unpublished reports of recent years, as well as current design practices, revealed the following.

Hydraulic

The discharge coefficient parameter plays the most significant role in any mathematical modeling of the landing gear. The dynamic loads on the airplane can vary over 25% with variation of C_d. The metering orifice is annular, with moving boundaries (conditions). The shape of the orifice is not the same during compression and expansion stroke. Therefore, the coefficient of discharge would be expected to be different for each of these two cases. Area of the metering pin has been neglected when writing the flow equation.

Although the snubbing valve acts as a one-way restrictor, the unrestricted flow of oil, during compression stroke, through holes in the upper bearing into the annular space between the cylinders generates a hydraulic force that should be added to the shock strut internal forces. During the extension stroke, the snubbing valve has been treated as a sharp edge orifice with a constant coefficient of discharge. Both of these assumptions are incorrect. The snubbing orifices as well as bearing holes are square-edged cylindrical capillary tubes, which may qualify as both small diameter pipes or thick length to diameter ratio orifices. The orifice discharge coefficient is essentially a function of Reynolds' number and orifice geometry and therefore would vary with stroke.

Pneumatic

No consensus exists as to the exact value of the polytopic exponent n. The very limited experimental data indicate that the effective polytropic exponent, for the air compression process, may be in the neighborhood of 1.1 for practical cases. A constant value of 1.1 has been used for n in the current simulation, although the subject needs a separate treatment.

Other Factors

Effect of the unsprung mass of the wheel assembly on the loads developed in the gear often has been neglected. All existing analyses and/or simulations have considered the initial impact condition only. The extension of the gear and

Description of Simulation

Figure 3 is a block diagram of the basic shock strut forces and how they interact in developing motion of the sprung and unsprung mass of the airplane. The simulation covers all of the models shown in this figure in considerable detail which also were developed by this author. The lift loss model makes it possible to simulate actual landings as well as drop tests by accounting for lift loss during spoiler deployment.

The combination of airplane and landing gear constitutes a system having two degrees of freedom (see Fig. 1), as defined by the vertical displacement of the sprung mass and the vertical displacement of the unsprung mass, which also is the tire deflection. The strut stroke S is determined by the difference between the displacement of the spring and unsprung mass by the angle between the axis of the strut and the vertical axis.

For inclined gears, compression of the shock strut produces a horizontal displacement of the axle. External lift forces corresponding to the aerodynamic lift are assumed to act on the system throughout the impact. In addition to the vertical forces, drag loads act between the tire and the ground.

The force inputs to these equations are a function of air compression, hydraulic resistance through cylindrical orifices, and variable area orifice, tire deflection characteristics, landing gear inclination, and wheel spin-up drag. Appropriate theoretical and semiempirical equations developed by Bell,[5,6] Schlichting,[7] and Knudsen, Davies, and Nootbar, et al.[8-10] were utilized to simulate the metering orifice discharge coefficient (C_{d_1}) variation. Similarly, equations developed by Merritt,[11] based on previous work by Langhaar,[12] Shapiro et al.,[13] and Kreith et al.[14] were utilized for simulating the snubber orifice discharge coefficient (C_{d_2}) variation. The basic equations of motion and equations for pneumatic force, internal friction force, ground reaction, etc., used in the simulation are based on the work of Milwitzky and Cook.[2] All of these equations, however, had to be modified, intersubstituted, and implicit techniques had to be used to convert them to analog form. Other major steps in achieving the simulation were as follows:

1) List information regarding strut geometry, tire characteristics, airplane sprung and unsprung masses, and so forth.

2) Assuming suitable scaling maximums, scale the equations.

3) Draw the computer diagram by use of standard practices (using ampliers to achieve the intended operation, e.g., division, multiplication, addition, function generation, and function limitation).

4) Use variable inputs, e.g., pin shape(s) and sink rates, to study the effect on other parameters, e.g. load stroke curves.

A summary of equations in the form used for the simulation follows.

Summary of Equations Used on Simulation

$$(\ddot{Z}_1) = (\ddot{Z}_2) + (\ddot{S})\cos\varphi \tag{1}$$

$$(\ddot{Z}_2) = g + \frac{\cos\varphi}{M_2}(F_s) - \frac{1}{M_2}(F_{vg}) + \frac{\sin\varphi}{M_2}(F_{Na}) \quad (2)$$

$$(\ddot{S}) = -\frac{(L)}{M_1}\sec\varphi + \frac{\sec\varphi}{M_2}(F_{vg}) - \frac{M_1+M_2}{M_1M_2}$$
$$\{(F_s) + (F_{Na})\tan\varphi\} \quad (3)$$

$$(F_s) = \frac{M_1M_2}{M_1+M_2}\left[-\frac{(L)\sec\varphi}{M_1} + \frac{\sec\varphi}{M_2}(F_{vg}\right]$$
$$-(F_{na}\tan\varphi \quad s=0 \quad (4)$$

$$(F_s) = (F_h) + (F_a) + (F_f) \quad s>0 \quad (5)$$

$$(F_a) = p_{a0}A_a(y) + F_s \quad \begin{matrix} s=0 \\ \leq F_{a0} \end{matrix} \quad (6)$$

$$(y) = n\frac{A_a}{v_0}\int \frac{(y)+1}{1-(A_a/V_0)(S)}(\dot{S})\,dt' \quad (7)$$

$$(F_{a0}) = p_{a0}A_a \quad (8)$$

$$(F_f) = \frac{\dot{S}}{|\dot{S}|}\ |F_{Na}|\left[(\mu_1+\mu_2)\frac{1_{2-(S)}}{1_{1+(S)}} + \mu_2\right] \quad (9)$$

$$(F_{Na}) = (F_{vg})\sin\varphi - (F_{Hg})\cos\varphi + \frac{W_2}{g}(\ddot{Z}_1)\sin\varphi - W_2\sin\varphi \quad (10)$$

$$(F_{vg}) = NK_\delta(Z_2) + NC_\delta(Z_2\dot{Z}_2) \quad (11)$$

$$(F_{Hg}) = (F_{v_g})(\mu_g) \quad (12)$$

$$(\mu_g) = f_5(R_r\omega) \quad (13)$$

$$(R_r) = R_0 - (Z_2/3) \quad (14)$$

$$(\omega) = \int \frac{F_{Hg})(R_T)}{I\omega}\,dt \quad (15)$$

$$(R_T) = R_0 - (Z_2) \quad (16)$$

$$(R_r\omega) = (R_r)(\omega) = V_{H0} \quad (17)$$

$$(F_h) = (F_{h1}) + (F_{h2}) \quad (18)$$

$$(F_{h1}) = (p_h - p_a)[A_1 - A_0 + (A_n)] \quad (19)$$

$$(p_h - p_a) = \frac{(Q_1)|Q_1|}{2(A_n)^2(C_{d1})^2} \quad (20)$$

$$(Q_1) = [A_1 - A_0 + (A_n)](\dot{S}) \quad (21)$$

$$(A_n) = (\pi/4)(\Delta D)(2D_0 - \Delta D) \quad (22)$$

$$(\Delta D) = f_1(s) \quad (23)$$

$$(1/c_{d1}^2) = (64/R_{e1}) + 2(f_p)(Z) + K \text{ compression only} \quad (24)$$

$$(R_{e1}) = [4\rho(Q_1)]/\{\pi\mu[2D_0 - (\Delta D)]\} \quad (25)$$

$$(f_p) = f_2(R_{e1}) \quad (26)$$

$$(Z) = 2L_1/(\Delta D) \quad (27)$$

$$K = f_3(Re_1/Z \quad (28)$$

$$[1/(C_{d1}^2)] = 2.25 + 2(f_p)(Z) - (F) \text{ extension only} \quad (29)$$

$$(F) = 1 - e^{-0.95(Z-1.15)} = f_4(Z-1.15) \quad (30)$$

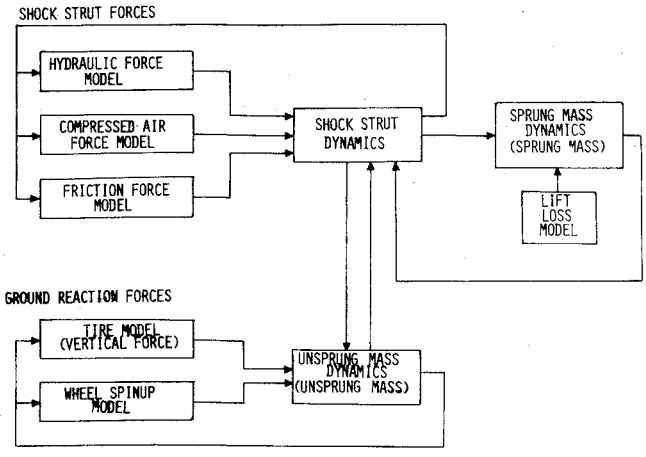

Fig. 3 Block diagram of shock strut simulation.

$$(F_{h2}) = (P_h - P_b)\frac{(A_2-A_1)^3(\dot{S})|\dot{S}|}{2A \text{ or comp.}^2\ C_{d2}^2} \text{ compression only}$$

$$A \text{ or } ex^2 \text{ extension only} \quad (31)$$

$$\frac{1}{(C_{d2})} = 1.5 + 13.74\left[\frac{\mu n_1 \pi L_{2c}}{4\rho[A_2 - A_1](\dot{S})}\right]^{1/2}$$

compression only

$$\mu n_2 \pi L_{2e} \quad \text{extension only} \quad (32)$$

The steps just preceding these equations are all part of standard procedure in formulating any analog simulation, and details therefore are not included. Moreover, the information used will vary from shock strut to shock strut.

Sample Resultss

Figures 4a and 4b show a sample output from the Brush Instrument Recorder plot for a medium jet airplane (model Y). It depicts the variation with strut stroke/time of important parameters, e.g., metering orifice coefficient (C_d), orifice Reynolds number (Re), snubbing orifice pressure (p_b), and internal friction force (F_f), along with other strut forces.

Correlation of Simulation Results and Test Data

In order to verify the performance predictions obtained from the computer, the known conditions of a physical landing gear drop test (model Y) were simulated. Time histories of both test and simulation results are given in the lower portion of Fig. 5 for two critical parameters. The correlation established the credibility of the simulation. No lift force has been simulated in the drop tests. Absence of lift was compensated for by reduction of the sprung mass.

An additional drop test correlation was made using a small jet (model X) landing gear. The basic difference in this test was that forces representative of wing lift were applied by means of pneumatic cylinders. A modification of the simulation was made to account for this effect. The data showing test and simulation results is included in the upper portion of Fig. 5 and again confirms the validity of the simulation.

Additional results from the simulation have been compared with drop test data and airplane landing data to establish the validity of the methods and equations used in the simulation. Figure 6 compares simulation results with drop test data for different metering pin shapes used on one of the modern jet transports. The maximum ground reaction force compares very well with test data for both of the pin shapes tested. Figure 6 also shows pressures inside the strut. These pressures are more sensitive to the internal characteristics of the strut than ground force, and therefore are good indicators as to

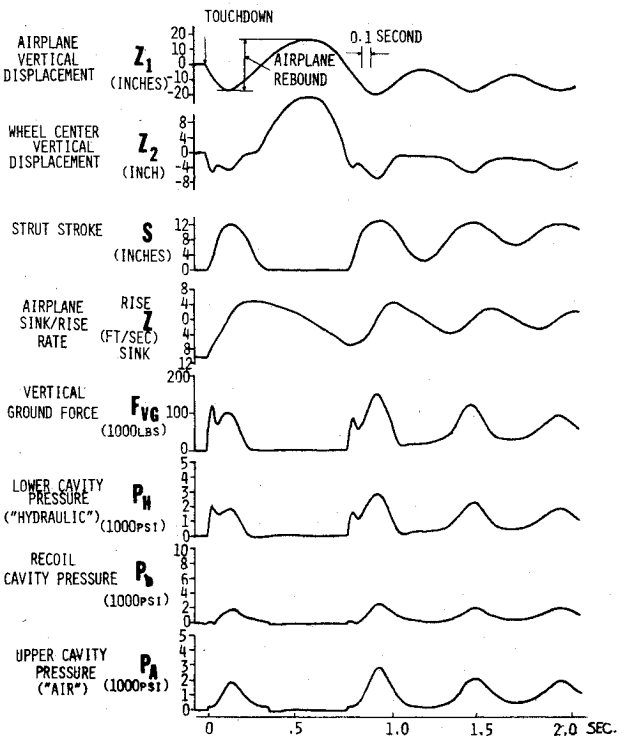

Fig. 4a Sample results.

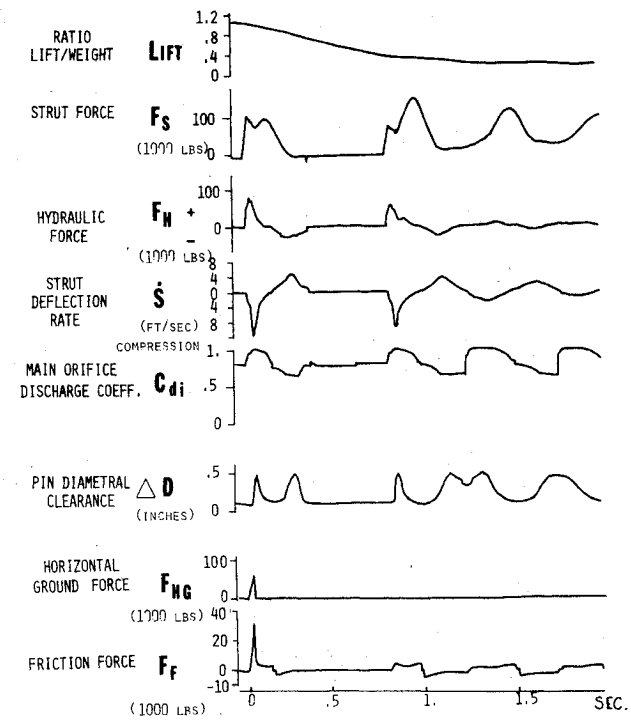

Fig. 4b Sample results.

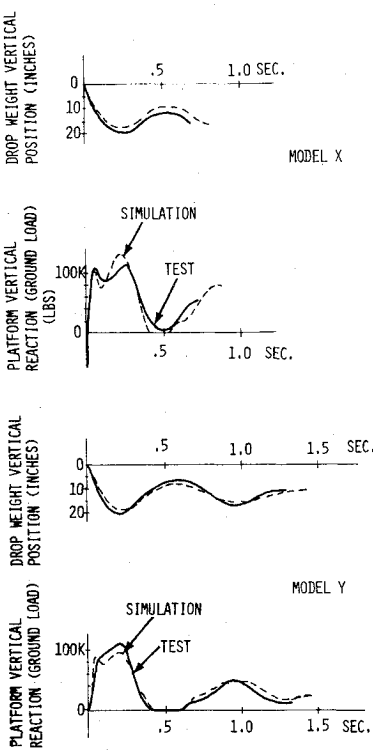

Fig. 5 Correlation of simulation results and test data.

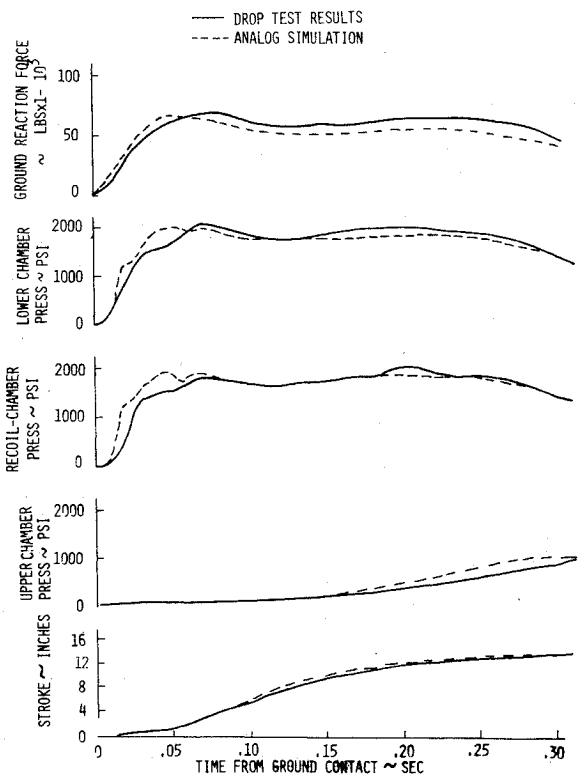

Fig. 6 Comparison of simulation and drop test results.

whether the internal forces in the strut are simulated accurately. The real proof of a shock strut simulation is whether it can predict the loads during an actual landing. Correlation is difficult because of the unknown or continuously changing parameters during actual flare and touchdown. Examples of these are as follows:

1) Variation of lift to weight ratio during the flare maneuver. This depends on pilot technique and will vary from landing to landing, even though the sink rate at touchdown might be the same.

2) Some airplane roll is normally present at touchdown, causing unsymmetrical force application to the shock struts on each side of the airplane. This effect can be accounted for in a simulation if both the left and right shock struts are simulated.

3) The time required to extend the spoilers or drag brakes will differ slightly from landing to landing.

Time history traces of shock strut position and incremental load factor are shown in Fig. 7 for the simulation and actual landing test results. The simulation and test data have the same trends, and the actual point to point correlation is considered to be good, especially in the the light of the variables in an airplane landing. The development and verification of the previously described shock strut simulation, along with its

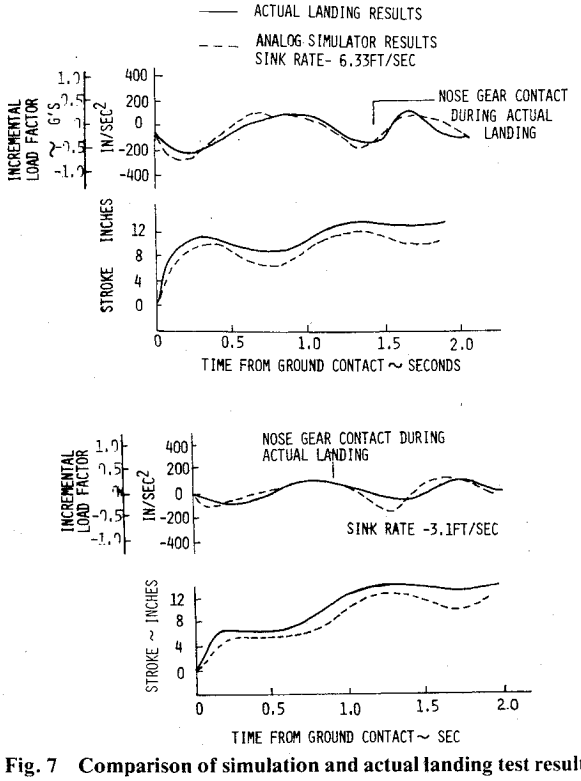

Fig. 7 Comparison of simulation and actual landing test results.

supporting digital setup and checkout programs, make it possible to proceed with confidence in the optimization of metering pin design.

Applications

Metering Pin Development

The metering pin is used in the shock strut to maintain a near-constant shock strut force during the stroke. A metering pin normally is designed for a landing impact corresponding to the maximum landing weight and the highest expected sink rate. The shock strut will be efficient in absorbing energy at this condition, but will not be optimum at other sink rates and airplane weights.

In the past, the design of metering pins has relied heavily on drop test results. It was not unusual for a number of pins to be drop-tested before one that produced the desired results was obtained. This procedure is very time-consuming and costly. The main impetus to develop a detailed shock strut simulation, which included a metering pin optimization technique, was to eliminate or minimize the need of drop tests as a development means.

A special circuit was devised on the analog simulation which allows the operator to vary the shape of the pin and observe the effects on shock strut load immediately. The analog simulation has the capability of high-speed, iterative operation (continuously repeating a run). This capability is used to repeat simulated airplane landings or drop-test runs at a rate of approximately 2/sec. The metering pin shape then can be continuously varied while the computer is in operation, and the resulting effect on the load/stroke curve can be noted on a scope. The use of an electronic memory scope makes it possible to compare a number of runs while altering the pin shape. An optimum metering pin can be developed for certain set of conditions in a relatively short time. Various parameters, such as sink rate, weight, or internal strut parameters, also can be varied to determine their effect on the load transmitted to the airplane. Figure 8 shows typical pictures of a scope display of the load/stroke characteristics for various sink rates and two different pin designs.

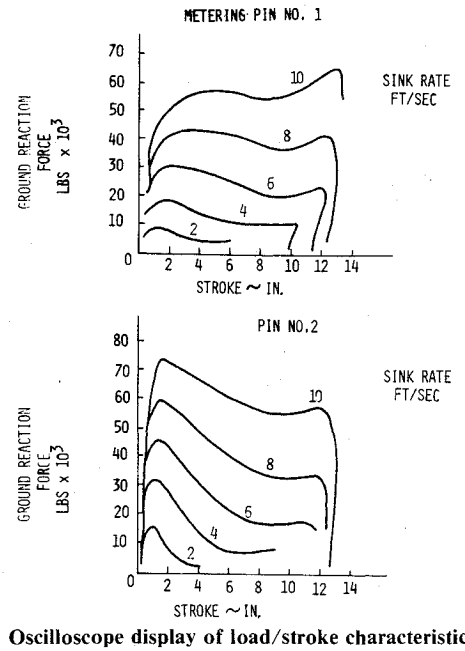

Fig. 8 Oscilloscope display of load/stroke characteristics at various sink rates (for two different pin designs).

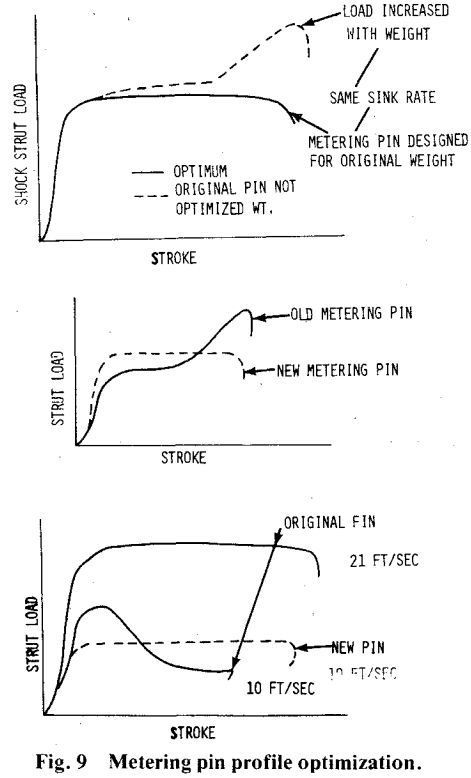

Fig. 9 Metering pin profile optimization.

Because of the optimization technique just described, once a new metering pin has been configured/optimized, tradeoff studies can be conducted to determine the effect of sink rate and aircraft weight on the shock strut force. At landing weights, in excess of that used to design the metering pin, the shock strut will not be operating at its highest efficiency, and the maximum load will increase by a larger percentage than the weight increase (see Fig. 9). The middle portion of Fig. 9 shows the type of gain that can be expected by redesigning the same metering pin for a higher gross weight aircraft. The lower portion of Fig. 9 shows a typical load stroke curve at sink rates of 10 and 21 fps for a metering pin designed at the higher sink rate. Also shown is a load stroke curve at 10 fps with a metering pin redesigned at this sink rate.

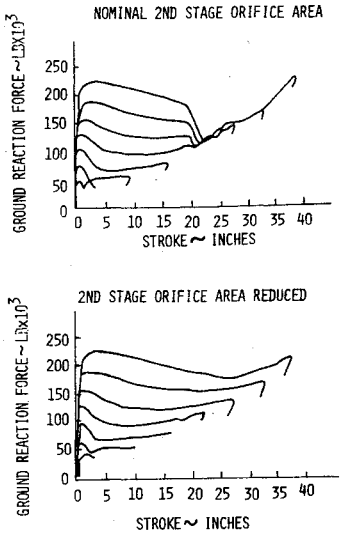

Fig. 10 Two-stage shock strut configuration.

Other Applications

Figure 10 shows the ground reaction force as a function of stroke for a typical two-stage shock strut. The advantages of such a shock strut are to 1) enable a high air compression ratio to be used, which reduces the energy stored in the compressed air and thus reduces rebound tendency, and 2) provide a relatively soft ride during taxi by keeping the air spring-constant low for the stroke position associated with taxi.

The performance of such a shock strut proposed for a modern supersonic airplane is depicted in the top half of Fig. 10 for sink rates of 2, 4, 6, 8, 10, 12, and 14 fps. The second stage comes into play at a stroke of 20 in., and there is an undesirable sudden drop in the reaction force. Studies conducted on the analog computer indicated that a smaller second-stage orifice would eliminate this sharp change in reaction force. The lower half of Fig. 10 shows the results of reducing the second-stage orifice from its nominal diameter of 3 in. to 0.85 in. This results in a smooth transition between the first and second stage, and would reduce some of the rebound tendency by dissipating more energy through hydraulic flow.

Conclusions

The development of metering pin shape in a typical oleo-pneumatic shock strut normally requires costly drop testing. The drop testing does not properly simulate airplane lift, drag, and wheel spinup. The use of accurate computer simulations has many payoffs, some of which are noted as follows:

1) Reduction or elimination of drop test costs.

2) Optimum design of metering pin profile, to enable minimum load multiplication, thus permitting an increased structural fatigue life.

3) Reduce-weight investment in gear support structure.

4) Enable inexpensive design of a family of pinshapes for incorporation into growth airplanes, or airplanes that see other than optimum load.

References

[1] Hurty, W.C., "A Study of the Response of an Airplane Landing Gear Using the Differential Analyzer," *Journal of the Aeronautical Sciences,* Vol. 17, Dec. 1950, pp. 756-764.

[2] Milwitzky, B. and Cook. F.E., "Analysis of Landing Gear Behavior," NACA Rept. 1154, 1953.

[3] Walls, J.H., "An Experimental Study of Orifice Coefficient, Internal Strut Pressures and Loads on a Small Oleo-Pneumatic Shock Strut," NACA TN 3426, 1955.

[4] Wojcik, C.K. and Mosco, C.A., "Determination of Metering Pin Profile for Prescribed Impact Loading of Airplane Landing Gear," American Society of Mechanical Engineers, Paper No. 68-Mech-50.

[5] Bell, K.J., "Annular Orifice Coefficients with Application to Heat Exchanges Design," Ph.D. thesis, Department of Ehcmical Engineering, University of Delaware, 1955.

[6] Bell, K.J. and Bergelin, O.P., "Flow Through Annular Orifices," *Transactions of the ASME,* April 1957, pp. 593-599.

[7] Schlichting, H., *Zeitschrift fur angewandte Mathematik und Mechanik,* Vol. 14, 1934, pp also reported in Goldstein, S., *Modern Developments in Fluid Dynamics,* Vol. I, Oxford University Press, New York, 1938, pp. 309-310.

[8] Knudsen, J.G. and Katz, D.L., "Fluid Dynamics and Heat Transfer," *Engineering Research Bulletin* No. 37, Engineering Research Institute, University of Michigan, Ann Arbor, Mich., 1953.

[9] Davies, S.J. and White, C.N., "An Experimental Study of the Flow of Water in Pipes of Rectangular Section," *Proceedings of the Royal Society of London, England, Series A,* Vol. 119, 1928, pp. 92-107.

[10] Nootbar, R.F. and Kintner, R.C., "Fluid Friction in Annuli of Small Clearance," *Proceedings of the Second Midwestern Conference on Fluid Mechanics,* Ohio State University Engineering Experiment Station Bulletin No. 149, 1952, pp. 185-199.

[11] Merritt, H.E., *Hydraulic Control Systems,* Wiley, New York, 1967, pp. 31-42.

[12] Langhaar, H.L., "Steady Flow in the Transition Length of a Straight Tube," *Journal of Applied Mechanics,* June 1942, pp.A55-A58.

[13] Shapiro, A.H., Siegel, R., and Kline, S.J., "Friction Factor in the Laminar Entry of a Smooth Tube," *Proceedings of the 2nd U.S. National Congress of Applied Mechanics,* June 1954, pp. 733-741.

[14] Kreith, F. and Eisenstadt, R., "Pressure Drop and Flow Characteristics of Short Capillary Tubes at Low Reynolds Numbers," *ASME Transactions,* July 1957, pp. 1070-1078.

[15] Hall, G.W., "Analytical Determination of the Discharge Characteristics of Cylindrical-Tube Orifices," *Journal of Mechanical Engineering Science,* Vol. 5, 1963, pp. 91-97.

[16] Lichtarowicz, A., Duggins, R.K., and Markland, E., "Discharge Coefficient for Incompressible Non-Cavitation Flow Through Long Orifices," *Journal of Mechanical Engineering Science,* Vol. 7, 1954, pp. 210-219.

[17] Kastner, L.J. and McVeigh, J.C., "A Reassessment of Metering Orifices for Low Reynolds Number," *Proceedings of the Institution of Mechanical Engineers,* Vol. 180, Pt. I, 1965-1966, pp. 331-356.

[18] Wojcik, C.K. and Mosco, C.A., "Determination of Metering Pin Profile for Prescribed Impact Loading of Airplane Landing Gear," American Society of Mechanical Engineers, Paper No. 68-Mech-50.